SUNSPOT ROTATION AND THE FIELD STRENGTHS OF SUBSURFACE FLUX TUBES

SYDNEY D'SILVA
Theoretical Astrophysics, Tata Institute of Fundamental Research, Bombay 400 005, India*

and

ROBERT F. HOWARD
*National Solar Observatory, National Optical Astronomy Observatories**, Tucson, AZ 85726, U.S.A.*

(Received 19 October, 1993; in revised form 22 January, 1994)

Abstract. Observations show that bipolar magnetic regions (BMRs) have differential rotation profiles that are faster than the local Doppler velocity profiles by about 5%, and the p-spots in the growing sunspot groups rotate faster than the f-spots. Also, the smaller spots rotate faster than the larger ones. We present detailed observations of the functional dependence of the residual rotation of sunspots on the spot size of the p- and f-spots of growing sunspot groups. Through numerical calculations of the dynamics of thin flux tubes we show that flux loops emerging from the bottom of the convection zone acquire a rotation velocity faster than the local plasma velocities, in complete contradiction to what angular momentum conservation would demand. The sunspot flux tubes need not be anchored to regions rotating faster than the surface plasma velocities to exhibit the observed faster rotation; we show that this occurs through a subtle interplay between the forces of magnetic buoyancy and drag, coupled with the important role of the Coriolis force acting on rising flux tubes. The dynamics of rising flux tubes also explains the faster rotation of smaller sunspots; we show that there is no need to evoke a radial differential rotation and anchoring of smaller spots to faster rotating regions. The simulated differential rotation profiles of the p- and f-legs of flux loops emerging in the convection zone, with a latitudinal differential rotation and velocity contours constant along cones, mimic the observed profiles for growing sunspot groups only when the flux loops emerge radially and obey Joy's law. (The 'legs' are defined to be the vertical part of the loops.) Also the rotation–size relation of growing sunspots is obeyed only by radially emerging loops which obey Joy's law. This constrains the fields at the bottom of the convection zone that are possible for producing the BMRs we see, to lie between 60 and 160 kG, which is in agreement with previous claims.

1. Introduction

It is believed that the dynamo operates at the bottom of the convection zone and that the magnetic features we see on the surface are produced by magnetic flux tubes generated in this region. These flux tubes have to traverse the entire convection zone before they appear at the surface and produce the magnetic features we see. They would mimic the butterfly diagram shown by the bipolar magnetic regions (BMRs) provided they emerge radially (emerge at the latitude from which they are released at the bottom of the convection zone). If the flux tubes at the bottom of the convection zone are weaker than 100 kG, the Coriolis force is so overwhelmingly

* This work was done at NOAO, while on leave from TIFR.

** Operated by the Association of Universities for Research in Astronomy Inc., under Cooperative Agreement with the National Science Foundation.

Solar Physics **151:** 213–230, 1994.

large compared to the magnetic buoyancy force, that they fail to emerge radially and appear at the typical sunspot latitudes (Choudhuri and Gilman, 1987; Choudhuri, 1989); instead, they move parallel to the rotation axis and appear at very high latitudes.

Flux tubes stronger than 100 kG have magnetic buoyancy strong enough to dominate over the Coriolis force and emerge radially. However, if they are stronger than 160 kG, they fail to obey Joy's law (D'Silva and Choudhuri, 1993, henceforth Paper I); they emerge so rapidly that they do not get enough time to be influenced significantly by the Coriolis force and produce the tilts (the tilt is the angle made by the line joining the two poles of a BMR with the local latitude at which it emerges) that are observed (Hale *et al.*, 1919; Wang and Sheeley, 1989, 1991; Howard, 1991). Weaker fields, up to the equipartition values of 10 kG, can also be made to obey Joy's law if they are brought out radially by special mechanisms which either dominate over or suppress the Coriolis force (D'Silva, 1993).

In this paper we investigate whether these fields, which emerge radially and obey Joy's law, also show the differential rotation exhibited by the BMRs (Howard, Gilman, and Gilman, 1984; Howard, 1990). In particular, we are interested in the observations of sunspots in growing sunspot groups (Howard, 1992a, henceforth Paper II; Howard, 1992b) because our calculations are for rising flux tubes. If the angular momentum of the flux tubes is conserved during their rise to the surface, then a simple calculation shown below, demands that those flux tubes which emerge radially from the bottom of the convection zone should have a rotation velocity which is 50% of the rotation velocity of the Sun. If Ω_{eq} is the equatorial rotation velocity of the Sun, assuming a solid body rotation and angular momentum conservation,

$$\Omega_{eq} r_0^2 \sin^2 \theta_{in} = \Omega R_\odot^2 \sin^2 \theta_{em} \,, \tag{1}$$

where Ω is the rotation velocity acquired by the flux tube when it reaches the surface, θ is the colatitude, and the subscripts in and em denote the initial and emerging values. A flux tube emerging from the bottom of the convection zone, at $r_0 = 0.7\, R_\odot$, to the surface, at $R_\odot$, will acquire an angular velocity $\Omega \approx 0.5 \Omega_{eq}$.

Contrary to what is expected, this happens only in the case of axisymmetric flux tubes, symmetric about the rotation axis (Choudhuri and Gilman, 1987; Moreno Insertis, 1986; Choudhuri and D'Silva, 1990; D'Silva and Choudhuri, 1991), or weak, non-axisymmetric flux tubes which are dominated by the Coriolis force (Choudhuri, 1989; D'Silva and Choudhuri, 1993; D'Silva, 1993). This situation is discussed in Section 3. The rotation velocity exhibited by the top portion of the emerging non-axisymmetric flux tubes is completely modified by the influence of magnetic buoyancy, magnetic tension, drag force and the special mechanisms which preferentially suppress or dominate over the Coriolis force. In Section 3 we show how the field strength and flux tube size affect the rotation velocity of the top of the flux loops. In Section 4 we study the differential rotation curves that the p- and f-legs of the flux loops exhibit when they emerge through the convection zone, which

has a latitudinal differential rotation as seen in the Doppler velocities at the surface (Snodgrass, Howard, and Webster, 1984) and has rotation velocities constant along cones as shown by the helioseismology results (Christensen-Dalsgaard and Schou, 1988; Dziembowski, Goode, and Libbrecht, 1989).

Observations show that BMRs rotate faster than the surrounding plasma by 5% (Howard, Gilman, and Gilman, 1984). On average, p-spots rotate faster than the f-spots (Gilman and Howard, 1985; Figure 5 of Paper II). Also, Howard, Gilman, and Gilman (1984) show that the large spots rotate slower than the smaller ones (see Figures 6 and 7 of Howard, 1992b). However, Paper II clearly shows that rotation depends very crucially on the evolutionary phase of the sunspot group. Table II of Paper II shows that growing spots rotate significantly slower than decaying spots. Figures 7 and 8 of Paper II show that p-spots rotate faster than f-spots by 3% in growing sunspot groups, whereas they rotate slower by 3% in decaying groups. In Section 2 we present a more detailed analysis of observations of growing sunspot groups. We show that both p- and f-spots show a decrease in residual rotation with increasing size.

We perform numerical calculations on thin flux tubes emerging from the bottom of the convection zone as in Paper I and find that in the absence of drag, if Coriolis force dominates over magnetic buoyancy, as in the case of 10-kG tubes, then the f- and p-spots rotate slower than the surrounding plasma, in addition to the fact that they appear at very high latitudes; calculations show that 10-kG tubes rotate slower than the surrounding plasma according to the simple calculations above. However, if the Coriolis force is suppressed or dominated over, then the tubes emerge at the sunspot latitudes.

The Coriolis force can be suppressed by increasing drag (decreasing the size of the flux tubes) or by increasing magnetic tension through decreasing footpoint separation (Paper I; D'Silva and Howard, 1993), or by angular momentum exchange of the tube with small-scale turbulence (Choudhuri and D'Silva, 1990; D'Silva, 1993). Essentially, Coriolis force is suppressed by reducing the rotation velocity of the loop v_ϕ. If the suppression is perfect, that is if the Coriolis force is reduced to zero, or in other words if $v_\phi = 0$ in the rotational frame, the spots produced by the tubes have rotation velocities close to that of the surrounding plasma. Magnetic buoyancy, however, would act to make the legs vertical, and hence in the process the p-leg would rotate faster and the f-leg slower than the local plasma velocity.

The Coriolis force can be dominated over by increasing magnetic buoyancy – that is by increasing the field strength of the flux loops (Choudhuri and Gilman, 1987; Choudhuri, 1989; Paper I), or if the updraught in giant cells drags the flux tubes (Choudhuri and D'Silva, 1990; D'Silva, 1993). If the Coriolis force is dominated over, however, v_ϕ is not equal to zero; it should be slower than the Doppler velocity profile as shown by the simple calculation above. Magnetic buoyancy plays a prominent role – it is surprising that it not only suppresses the 50% slower rotation velocity that angular momentum conservation demands, but also gives a boost to the flux loop in the direction of rotation, giving the f- and

p-spots produced by the loops a rotational velocity faster than the local Doppler velocity. The process is a subtle interplay between Coriolis force and magnetic buoyancy. If the flux loop moves 'sufficiently slowly' in the initial stages of its emergence, then the Coriolis force helps to drain the fluid in the p-leg of the flux loop to the f-leg in the near-horizontal portion of the flux loop, which is the top portion of the flux loop (because the effect of Coriolis force on the fluid in the vertical portion of the loops (the legs) is to push the flux loop as a whole in the negative ϕ direction). This intensifies the field strength of the p-leg and hence its magnetic buoyancy (Fan, Fisher, and DeLuca, 1993). Thus the p-leg emerges rapidly, dragging with it the f-leg, and they both gain a rotational velocity faster than the Doppler velocity. We can quantify 'sufficiently slowly' by adjusting the initial values of field strength, flux tube size, footpoint separation and anchoring mechanisms. This can put constraints on these initial values, because not only should the flux tube emerge radially at the sunspot latitudes, it should also obey Joy's law, and in addition should show the right differential velocities and the functional dependence of the differential velocities with size.

We find that for fields weaker than 60 kG the p-legs rotate slower than the f-legs (Figure 3(c)), contrary to the observations. They also rotate much slower than the surrounding plasma. It is unlikely that these weak equipartition fields, weaker than 60 kG can produce the BMRs we see; not only do they fail to emerge radially, they disobey Joy's law (Paper I) and do not show the observed differential rotation profiles, unless the special mechanisms (Choudhuri and D'Silva, 1990; D'Silva, 1993) of suppressing or dominating the Coriolis force are in play.

All fields stronger than 60 kG, regardless of size, show that the p-legs rotate faster than the f-legs. However, only in the range of 60 to 160 kG, where they emerge radially and obey Joy's law, do they exhibit differential rotation profiles very close to the observed ones. In all other cases, the differential rotation profile is significantly different than the observed profile. In particular, if megagauss fields were responsible for producing the sunspots, then the p-spots would rotate twice as fast as the plasma and the f-spots would rotate in the opposite direction. Also, though the f-spots show a decrease in residual velocity with increasing size, the p-spots behave in exactly the opposite fashion. This gives very strong evidence against the presence of megagauss fields at the bottom of the convection zone, and reconfirms the results of Paper I – the fields responsible for producing the sunspots should lie roughly between 60 and 160 kG.

In the next section, we present the analysis of the observations for growing sunspot groups. The numerical results of the dynamics of flux tubes rising in a convection zone with solid body rotation are given in Section 3. In Section 4 we present the differential rotation profiles of the f- and p-spots produced by the emerging flux loops in a differentially rotating convection zone. In Section 5 we discuss the dependence of rotation velocity of the spots on size and in Section 6 we present the conclusions.

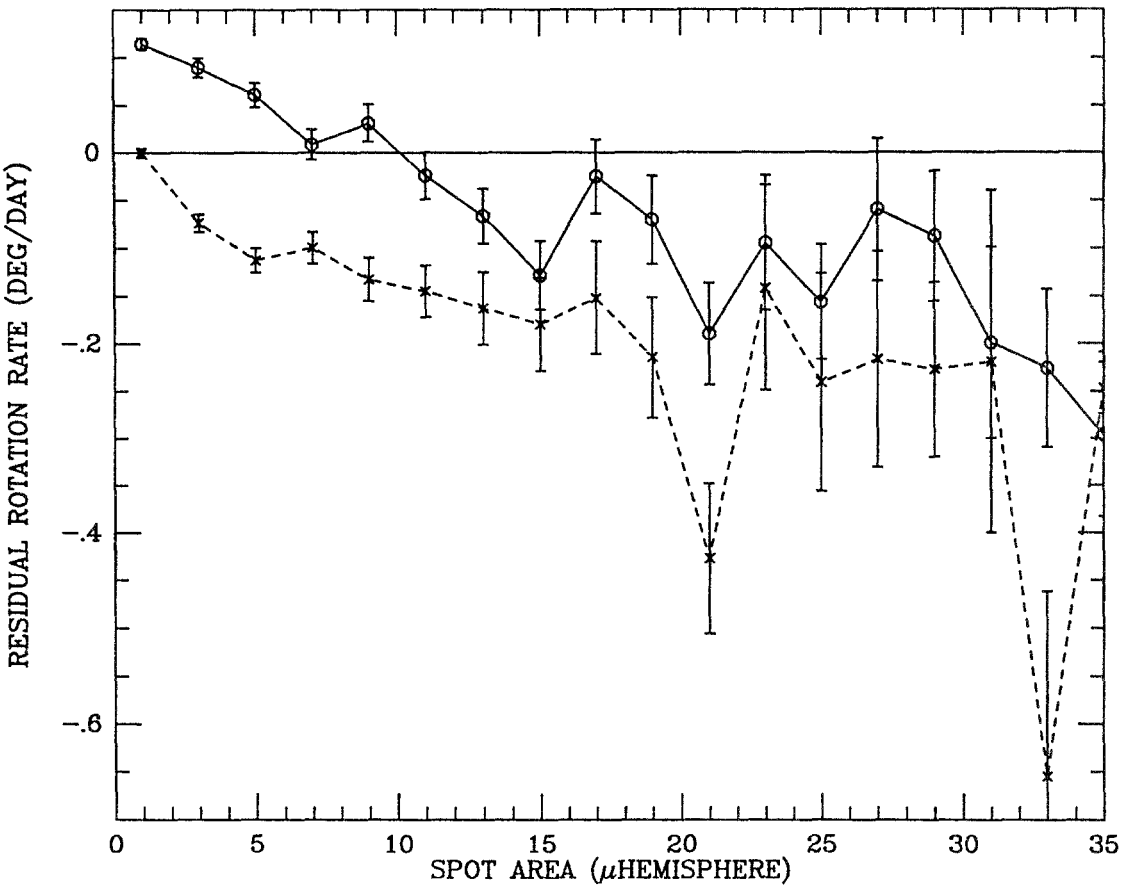

Fig. 1a. The relationship of the residual rotation rate with the spot area for the p- and f-spots for all sunspots.

2. Observations

Observations (Figure 3 of Howard, Gilman, and Gilman, 1984) show that on average sunspots and sunspot groups rotate faster than the local plasma. Also small spots rotate faster than larger ones (Figure 4 of Howard, Gilman, and Gilman, 1984). The residual rotation rate (which is the difference between the measured rotation velocity and the average rotation velocity of the spots at a particular latitude) is shown to decrease with spot size (Figures 6 and 7 of Howard, 1992b); for spots, the residual rotation rate – spot area curve has a slope of $-0.0131 \pm 0.00035°$ day^{-1} μhemisphere^{-1}.

Paper II shows that the rotation rate depends on whether the spot belongs to the following or preceding portion of the sunspot group. Figure 1(a) shows the residual rotation with size of the sunspot in μhemisphere, where 1 μhemisphere is 3.06×10^{16} cm^2, which is roughly equivalent to a radius of 1000 km. The solid line

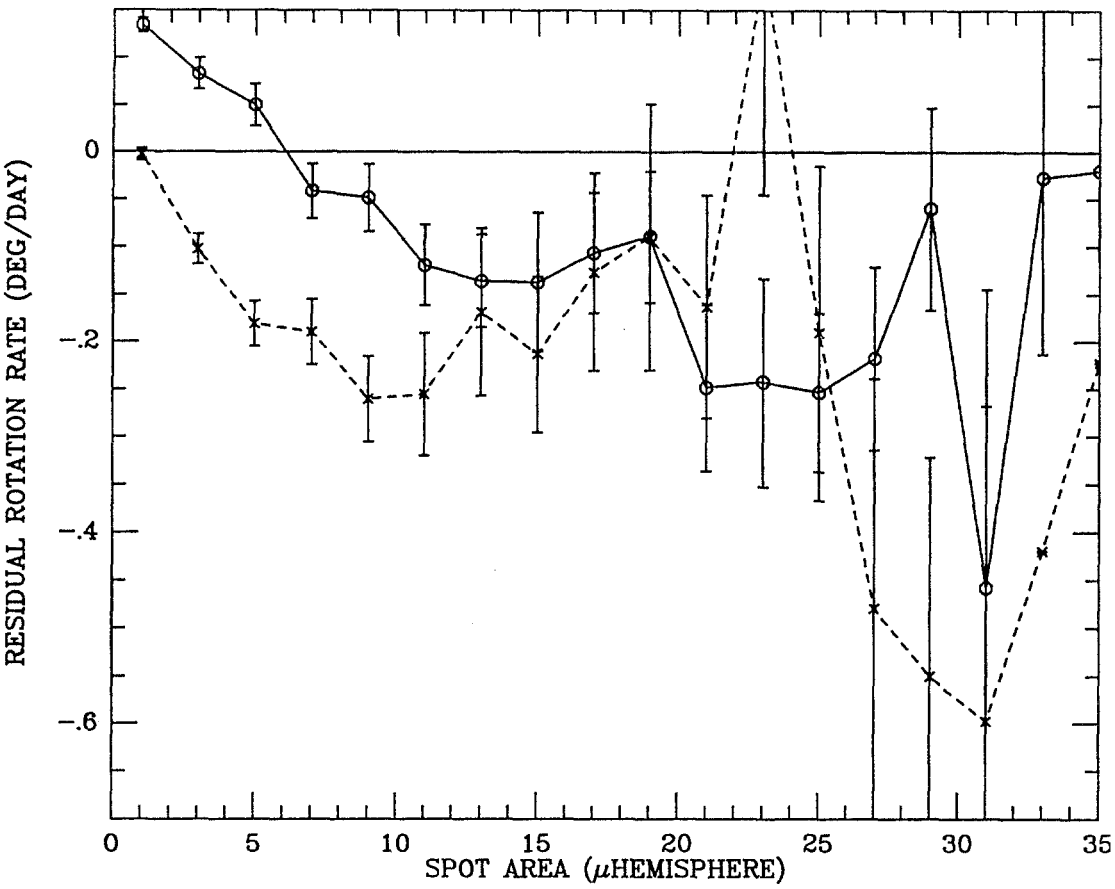

Fig. 1b. Same as Figure 1(a), except for growing spot groups.

is for the p-spots and the dashed line is for the f-spots. Here the residual rotation is the difference between the measured rotation velocity and the average rotation velocity of the spots given by

$$\Omega = A + B \sin^2 \lambda + C \sin^4 \lambda \,, \tag{2}$$

where λ is the latitude and the coefficients $A = 14.38°$ day^{-1}, $B = 2.904°$ day^{-1}, and $C = 0$. (The numerical calculations below use $A = 14.1°$ day^{-1}, $B = -1.7°$ day^{-1}, and $C = 2.35°$ day^{-1}.) Note that the p-spots of any given size rotate faster than the f-spots of the same size, so that the p-curve is above the f-curve.

Paper II and a number of other studies (see references and discussion in Paper II) clearly show that the rotation rate depends upon the evolutionary phase of the sunspot group. Figure 1(b) shows the residual rotation of the sunspots for the growing sunspot groups. Note that the curves are steeper than those for all sunspots which are growing and decaying. The slopes from least-squares fits for all groups are $-0.012 \pm 0.001°$ day^{-1} μhemisphere^{-1} for p-spots and $-0.019 \pm 0.001°$ day^{-1}

μhemisphere^{-1} for f-spots (Figure 1(a)). For growing groups (Figure 1(b)) the slopes are $-0.022 \pm 0.002°$ day^{-1} μhemisphere^{-1} for p-spots and $-0.035 \pm 0.002°$ day^{-1} μhemisphere^{-1} for f-spots. These slopes are calculated using only the points on the left of the figures (0–12 μhemisphere).

3. Results for a Convection Zone with Solid Body Rotation

We model the flux tube as a one-dimensional string using the dynamical equations of Spruit (1981). The basic equations for a non-axisymmetric flux ring were derived in Choudhuri (1989) and are given in Paper I. Here we use all the equations, initial conditions, description of the ambient medium and code as in Paper I. (In Section 4 the ambient medium has a differential rotation as described there.)

We first set the drag term $D = 0$. A flux tube of initial field strength $B_0 = 10$ kG is released at a latitude of $\lambda_{in} = 5°$ at the bottom of the convection zone. Equations (5)–(7) of Paper I are integrated for a zero initial velocity and $m = 4$ (m is the number of loops per flux ring). The portion of the flux loop above the bottom of the convection zone rises due to magnetic buoyancy. The Coriolis force is large compared to magnetic buoyancy and the tube emerges at a very high latitude of $\lambda_{em} = 45°$ with a negative tilt (Figure 6(b) of Paper I). The filled circles in Figure 2(a) show the final configuration of the flux tube in the $r - \phi$ plane when its top hits the top of the convection zone. The open circles show the angular velocity of each point along the tube in the rotating frame of the Sun in units of its angular velocity. Note that the entire flux tube rotates in the negative ϕ direction in the rotating frame. In other words, the angular velocity exhibited by these 10-kG tubes would be smaller than that of the Sun, giving a rotation period longer than that of the plasma. In Equation (1), $\theta_{em} = 45°$, $\theta_{in} = 5°$, $r_0 = 0.7\,R_\odot$, giving $(\Omega/\Omega_{eq}) = 0.973$. In the rotating frame $(\Omega/\Omega_{eq}) = (1 - 0.973) = 0.027$, which is roughly the angular velocity shown by the top of this 10-kG flux loop.

Figures 2(b) and 2(c) are identical to Figure 2(a), except that the initial field strength B_0 is 100 kG and 1000 kG, respectively. Magnetic buoyancy tries to straighten out the legs of the flux loop to make them vertical. In the process of doing so, the p-leg of the 100-kG flux loop rotates faster than the plasma velocity by 10% and the f-leg is slower by 10%. The p-leg of the 1000-kG flux loop rotates more than 100% faster than the plasma velocity, giving a rotation period which is less than 15 days, and the f-leg rotates more than 200% slower than the plasma velocity! The magnetic buoyancy force is so overwhelmingly large that the legs, in the process of straightening up due to buoyancy, get an extremely large azimuthal velocity in directions opposite to each other. Besides the fact that megagauss fields do not obey Joy's law (Paper I), this is a very strong reason to rule out the presence of megagauss fields at the bottom of the convection zone.

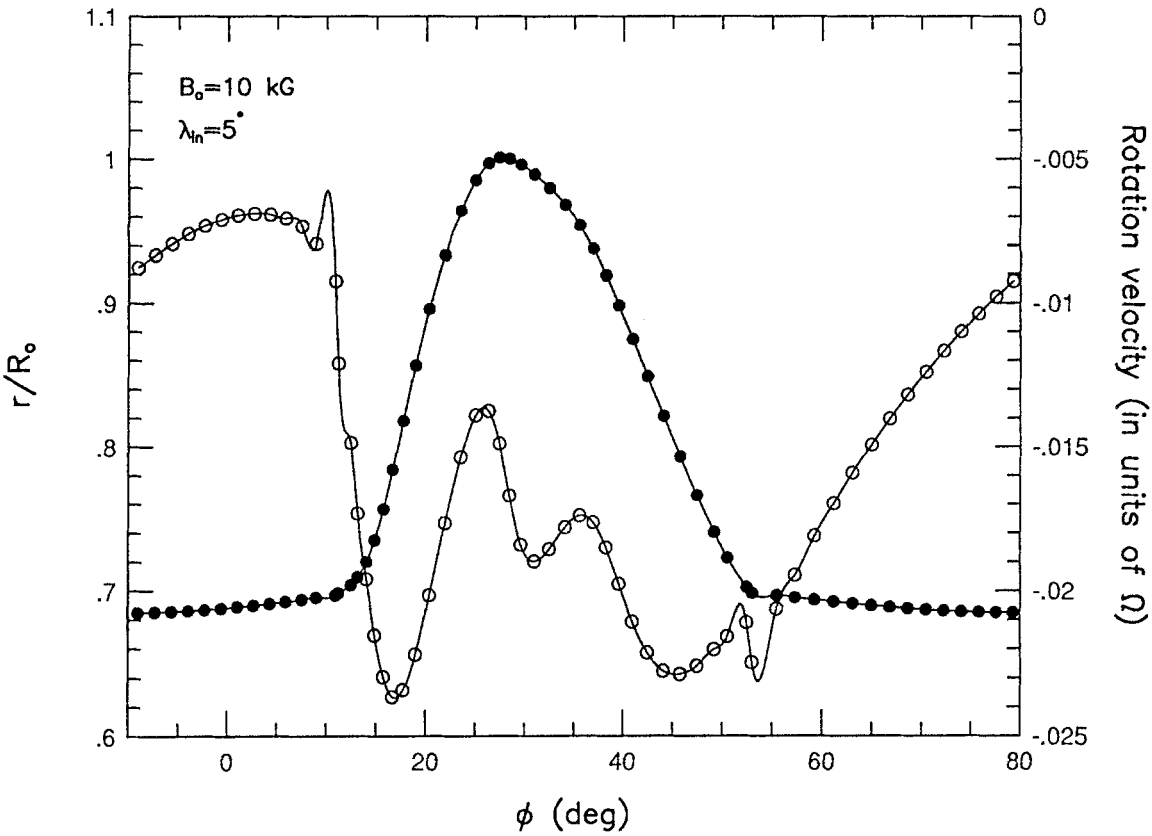

Fig. 2a. The final configuration of a 10-kG flux loop released at 5° latitude at the bottom of the convection zone which is rotating like a solid body (filled circles) in the $r - \phi$ plane. r is in the units of $R_\odot$. The open circles represent the rotation velocity in the rotating frame along the loop in units of rotation velocity of the Sun. A positive value indicates a rotation faster than the plasma velocity.

4. Results for a Differentially Rotating Convection Zone

Helioseismology observations show that the contours of constant Ω lie on cones (Christensen-Dalsgaard and Schou, 1988; Dziembowski, Goode, and Libbrecht, 1989). The surface Doppler velocity profile (Howard and Gilman, 1984; Snodgrass, Howard, and Webster, 1984) is given by Equation (2) with the coefficients $A = 14.1°$ day^{-1}, $B = -1.7°$ day^{-1}, and $C = -2.35°$ day^{-1}. We assume that the contours of constant Ω lie in cones in the convection zone with the latitudinal dependence given by the surface Doppler velocity profile. We incorporate the Lagrangian derivative of Ω,

$$\frac{\mathrm{d}\Omega}{\mathrm{d}t} = \frac{\partial \Omega}{\partial t} + \mathbf{v} \cdot \nabla \Omega = 2B \sin\lambda \cos\lambda + 3C \sin^3\lambda \cos\lambda \,, \tag{3}$$

on the left-hand side of Equation (7) of Paper I as described in the Appendix of Paper I, and assume $\Omega(\theta)$ as in Equation (2).

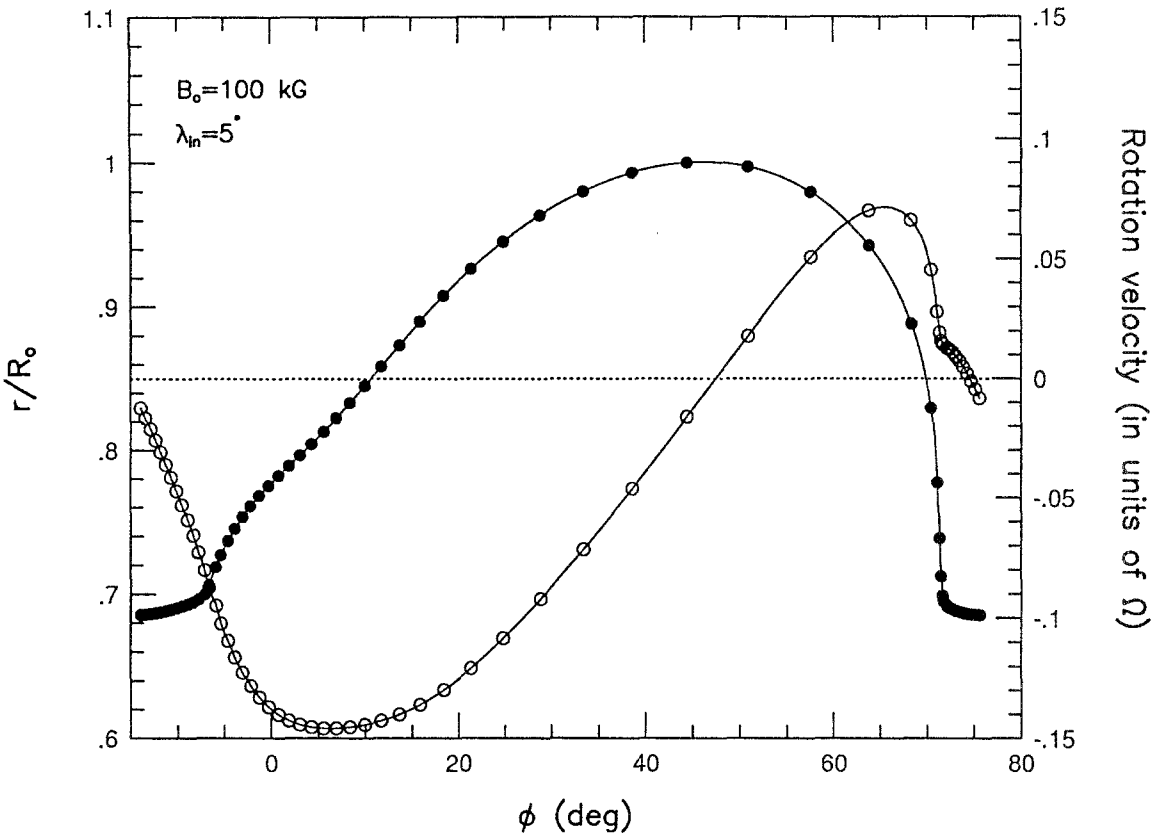

Fig. 2b. Same as Figure 2(a) for a 100-kG flux loop.

A megagauss flux tube is released from a latitude of 5° at the bottom of the convection zone. The drag is assumed to be zero, and $m = 4$. We integrate Equations (5)–(7) of Paper I after incorporating the differential velocity profile. The rotation velocities of the p-leg and f-leg at a depth of 0.95 $R_\odot$ are measured and plotted in Figure 3(a). The filled circles represent the rotation velocity of the f-leg, Ω_f, and the open circles that of the p-leg, Ω_p. The solid curve is the Doppler velocity profile of Equation (2). The calculations are repeated for flux tubes released at $\lambda_{in} = 10°, 20°, 25°, 30°$, and 35°; Ω_p and Ω_f are calculated. The dot-dashed line in Figure 3(a) shows the differential velocity profile of the p-spots and the f-spots. The p-spots rotate twice as fast as the local plasma and show a differential rotation profile opposite to the plasma differential rotation, just as for the solid body rotation case in Figure 2(c). The Ω_f profile shows that the f-spots rotate in the opposite direction to the rotation of the Sun.

Magnetic buoyancy dominates the dynamics of these flux tubes. The p- and f-legs of the flux loop try to become vertical due to this effect, and hence have extremely large velocities in the opposite directions, giving the p-spot a large

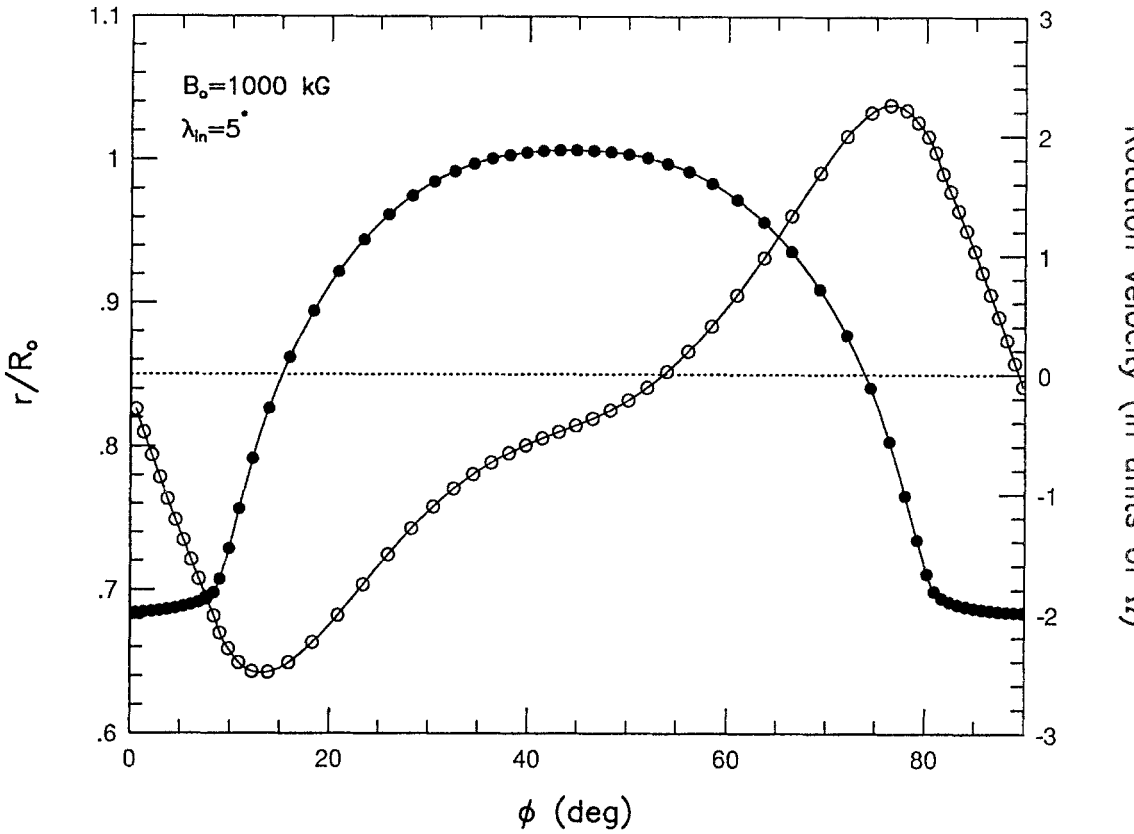

Fig. 2c. Same as Figure 2(a) for a 1000-kG flux loop.

positive rotation velocity and the f-spot a large negative rotation. Drag can reduce these velocities. So we incorporate drag in the equations and integrate them for the same initial conditions as for the no-drag case, and calculate the differential velocity profiles. The short dashes and long dashes show the differential velocity profiles when drag is incorporated. The short dashes represent 100 km flux tubes and the long dashes are for the 1000 km flux tubes. The rotation profiles approach the Doppler velocities when the flux tube size is decreased (drag is increased). However, even for the 100-km tubes, the f-spots rotate slower than the Doppler velocities by 25%, but the observations show that all spots rotate faster than the Doppler velocity values at all latitudes by roughly 5%. Clearly, this is further strong evidence against the presence of megagauss fields at the bottom of the convection zone.

The calculations are repeated for 100-kG tubes of various sizes and the results plotted in Figure 3(b). The differential velocity profiles approach the Doppler velocity profiles; the Ω_p profiles are only 7 to 10% faster and the Ω_f profiles are slower than the Doppler velocities (except for the 100 km tubes, which more or

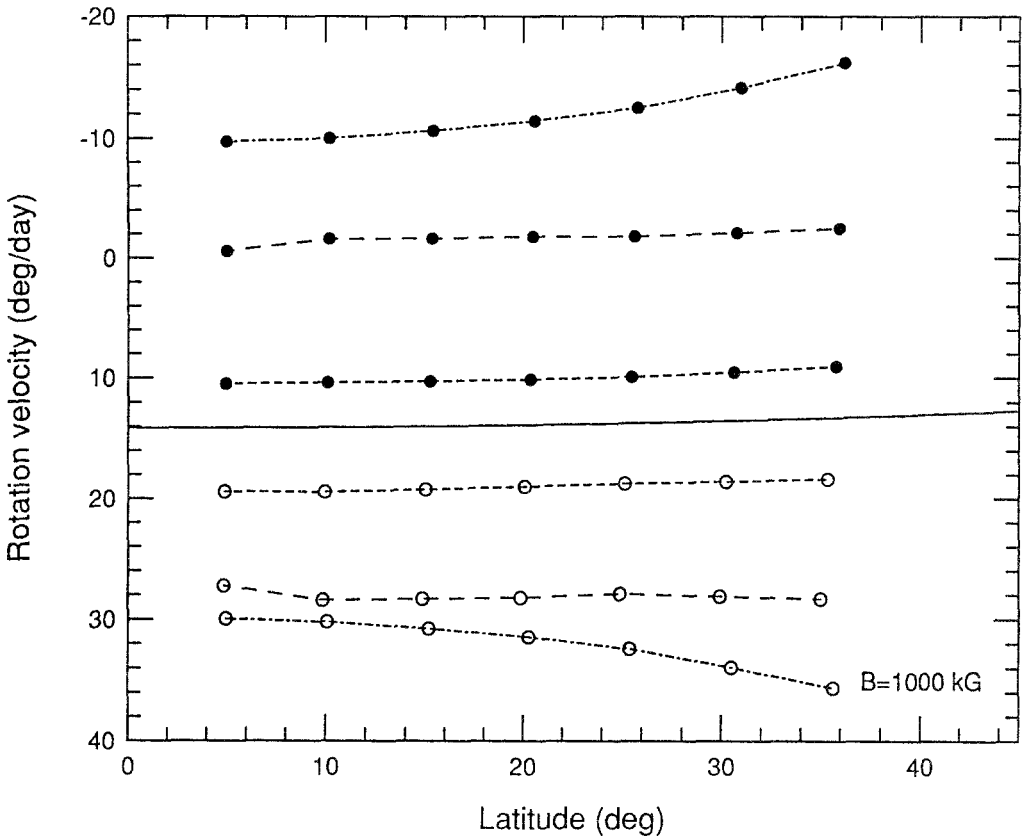

Fig. 3a. The open circles (filled circles) represent the rotation velocity of the p-leg (f-leg) of the flux loop in its final configuration when its topmost portion hits the top of the convection zone at a radius of 0.95 $R_\odot$, for flux loops of 1000 kG released at 5°, 10°, 15°, 20°, 25°, 30°, and 35° latitude at the bottom of a differentially rotating convection zone. The solid line represents the latitude dependence of the rotation velocity of the convection zone given by Equation (2). The short dashes are for 100 km and long dashes for 1000 km flux tubes. The dot-dashed line is for flux tubes in which the drag term is reduced to zero.

less show the Doppler profile). It is interesting to note that these 100-kG flux tubes not only emerge radially from the bottom of the convection zone and obey Joy's law, they also show differential rotation profiles close to the observed ones.

Fields weaker than 60 kG show differential rotation profiles slower than the Doppler profiles. Figure 3(c) shows the example of 30-kG flux tubes. Note that here the f-spots rotate slightly faster than the p-spots, in complete contradiction to the observations.

The rotation profiles of these fields approach the observed ones when they are made to emerge radially by the special mechanisms of giant cell drag or angular momentum exchange (Choudhuri and D'Silva, 1990; D'Silva and Choudhuri, 1991; D'Silva, 1993). Figure 3(d) shows an example for the angular momentum exchange mechanism acting on a 30-kG flux tube. As the angular momentum ex-

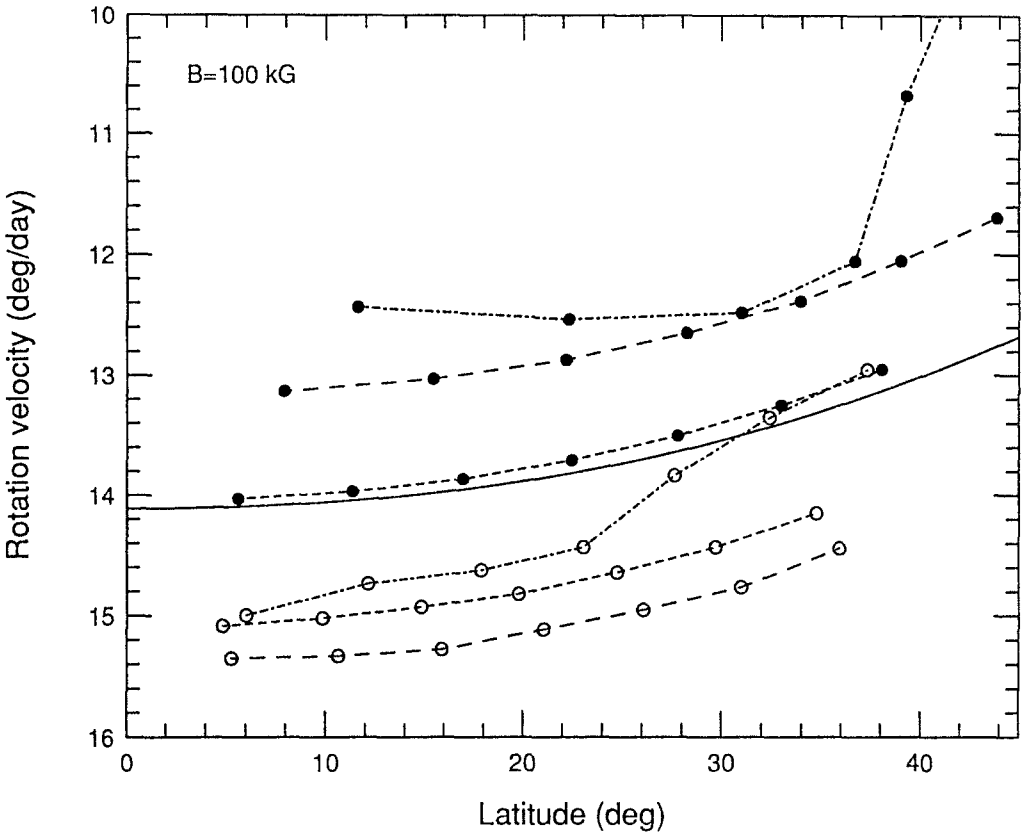

Fig. 3b. Same as Figure 3(a) for 100-kG flux tubes.

change time, τ, decreases, that is, when the efficiency of the angular momentum exchange process increases, the flux tubes emerge radially, obey Joy's law (Figure 5(a) of D'Silva, 1993), and also show differential rotation profiles close to the observed values with the p-spot rotating faster than the f-spot.

5. Size Dependence of Ω

We calculate the residual rotation for the p- and f-legs of megagauss flux tubes of various sizes released at $\lambda_{in} = 5°$. The results are plotted in Figure 4(a). The f-spots show a decrease in velocity with size, as expected. The p-spots show the opposite trend, in addition to the fact that both the plots are nowhere close to the observed values.

Figure 4(b) shows the residual rotation as a function of size for 100-kG tubes. This quantity shows a decrease in residual rotation with size in almost the entire range of the parameter space, for both the p- and f-spots, though these values differ from the observed values (compare with Figure 1(b)).

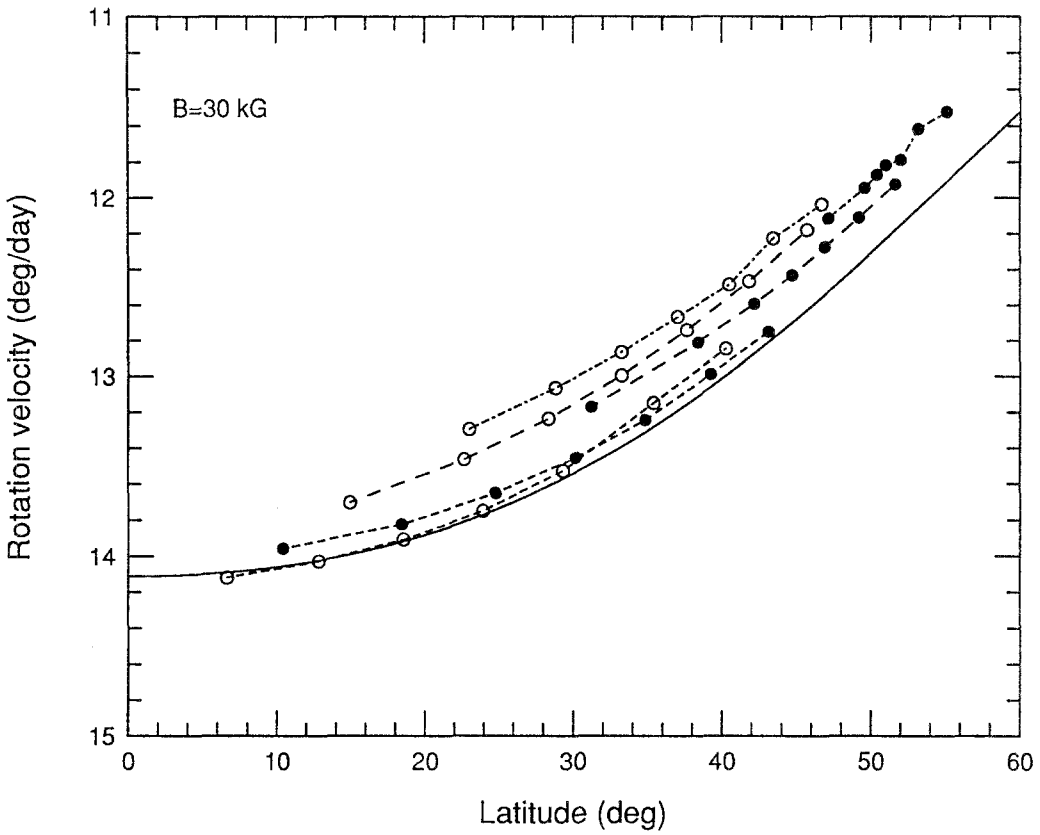

Fig. 3c. Same as Figure 3(a) for 30-kG flux tubes.

The 30-kG flux tubes in Figure 4(c) show that the residual rotation decreases with increasing size. However, the f-spots rotate faster than the p-spots for $\sigma_0 >$ 1000 km, contrary to the observations.

6. Conclusions

There have been numerous suggestions in the literature to explain the high rotation rate of sunspots: sunspots could preferentially be generated in those convection cells whose azimuthal velocities in the rotating frame of the Sun are in the direction of rotation (Yoshimura, 1971), or the flux tubes of the sunspots could be anchored to regions which are rotating faster than the surface Doppler velocities (Foukal, 1972); a radial differential velocity increasing with depth could also explain the increase in rotation rate with spot size, if spots of larger sizes are anchored to slower rotating regions than the small spots (Gilman and Foukal, 1979). Here we have shown that even in the absence of such phenomena the effect of a combined interplay of Coriolis force with magnetic buoyancy, drag and magnetic tension can

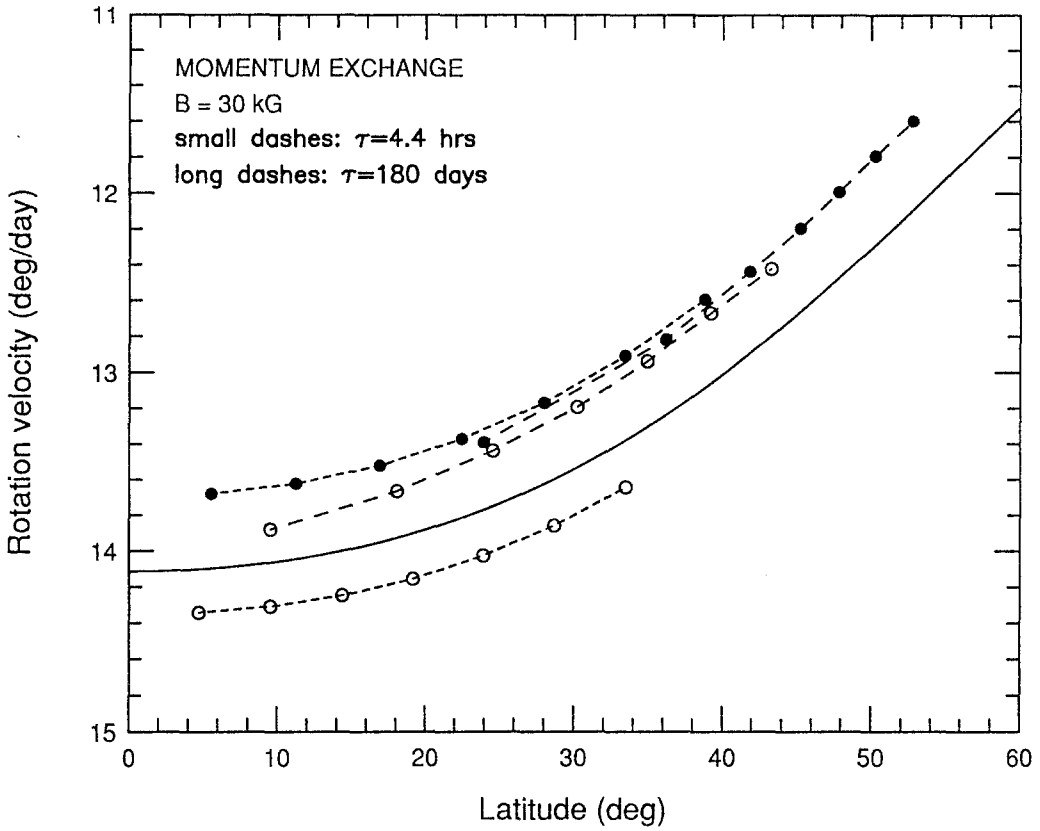

Fig. 3d. Same as Figure 3(a) for 30-kG flux tubes which are made to emerge radially with the angular momentum exchange mechanism.

mimic the observed differential rotation profiles.

Magnetic buoyancy tries to straighten up the legs of the emerging flux loop and make them vertical. In this process the p-leg acquires a positive rotation velocity faster than the local plasma rotation and the f-leg a negative velocity, thus explaining why p-spots of the growing sunspot groups rotate faster than the f-spots as observed (Paper II; Figure 3) by 3%. The Coriolis force acting on these emerging flux loops provides an asymmetry which makes the p-leg more buoyant, and hence it acquires a larger positive azimuthal velocity and pulls the f-leg (that is the entire loop) with it, giving the whole loop a net rotation velocity faster than the local plasma. This asymmetry is created when the plasma drains out of the p-leg by the mass flow induced by Coriolis force in the horizontal regions of the loop. This mass flow from the p-leg to f-leg evacuates the p-leg and makes it magnetically more buoyant than the f-leg. This evacuation can occur during the initial stages of the rise of the loop when the curvatures of the loop are small, provided the flux loop rise is slow enough to give the Coriolis force enough time

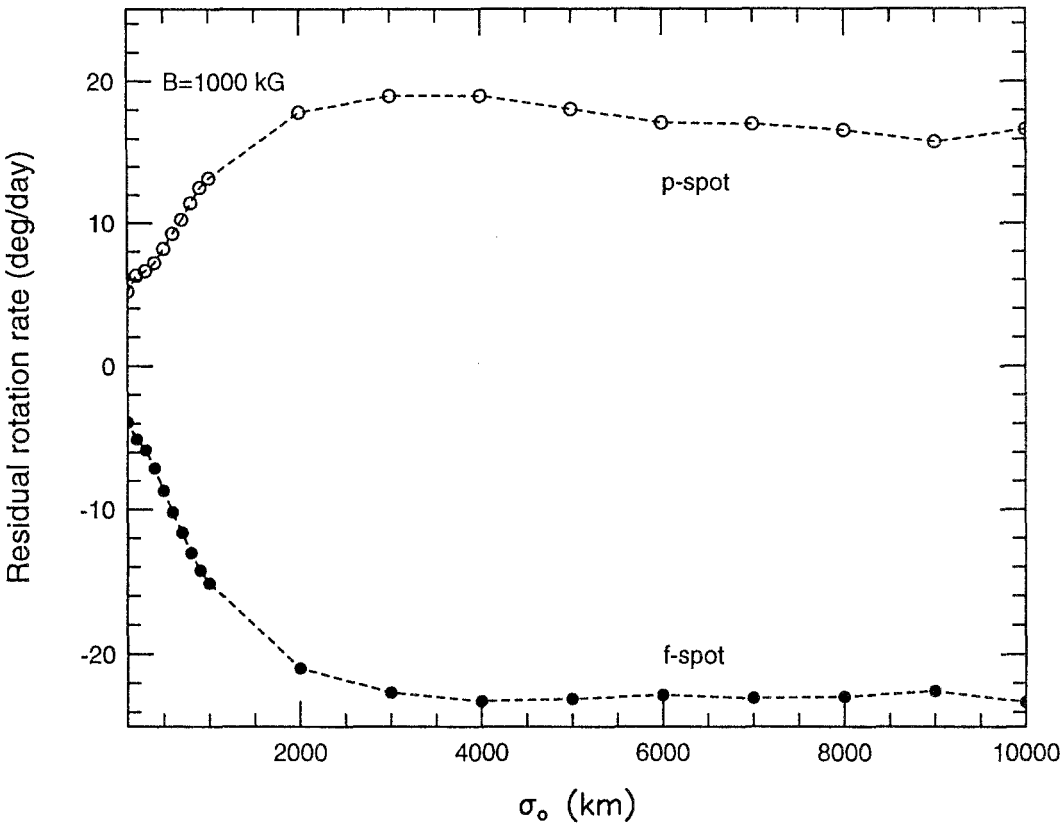

Fig. 4a. The residual rotation rate which is the difference of the rotation velocity of the p-leg (open circles) and the local Doppler velocity given in Equation (2), for 1000-kG tubes released at 5° latitude in a differentially rotating convection zone for different flux tube sizes.

to interact. Megagauss fields, because of their large buoyancy, emerge rapidly to the surface from the bottom of the convection zone, giving no time for the Coriolis force to interact with the tube in evacuating the p-leg. Figure 2(c) clearly shows the perfect symmetry in the final configuration of the flux tube and the rotation velocity distribution. Fields in the vicinity of 100 kG rise sufficiently slowly so that the p-leg is evacuated, giving rise to an asymmetry in the rise of the flux loop (as clearly seen in Figure 2(b)). These flux loops not only emerge radially, they also obey Joy's law (Paper I) and rotate faster than the surrounding plasma. The Coriolis force overwhelms the magnetic buoyancy of equipartition fields, and they move parallel to the rotation axis to emerge at very high latitudes. They fail to obey Joy's law (by showing negative tilts; Figure 6(b) of Paper I) and also rotate slower than the surrounding plasma (Figure 2(a)).

The faster rotation of smaller spots compared to larger ones (Howard, Gilman, and Gilman, 1984) has been explained by assuming that the smaller spots are

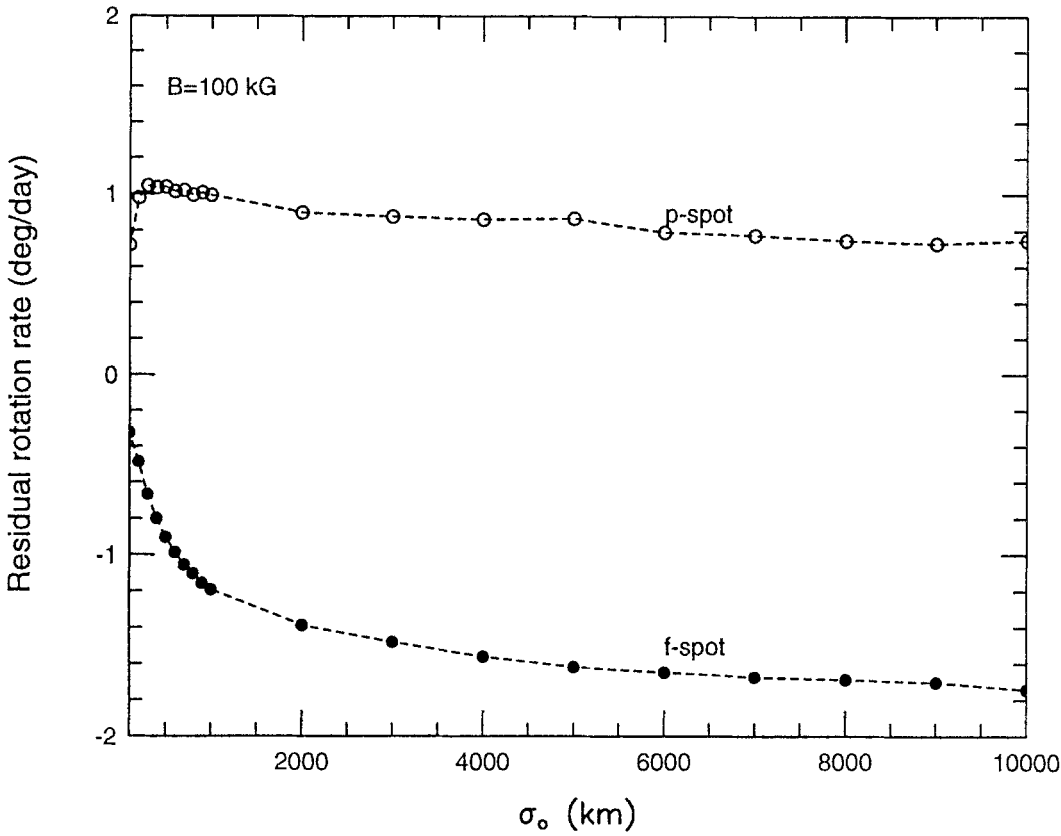

Fig. 4b. Same as Figure 4(a) for 100-kG flux tubes.

probably anchored to regions that rotate faster than the regions to which larger spots are anchored (Gilman and Foukal, 1979). Other explanations involve the well-established result that young spot groups rotate faster than older ones (which is contested by Howard, 1992a): if the smaller spots are young ones, then this qualitatively explains the size dependence of the rotation rates. However, the results of this study suggest another explanation. Drag varies inversely as the size of the flux tube. Drag on the large flux tubes is less than on the smaller ones; they emerge faster, giving less time for Coriolis force to act and evacuate their p-legs. Hence large flux tubes get less of a boost in the direction of rotation than do the smaller tubes. This explains the decrease in rotation rate with increasing size (Howard, Gilman, and Gilman, 1984; Paper II; Howard, 1992b).

Flux tubes between 60 and 160 kG have a magnetic buoyancy which is just the right magnitude to counteract the Coriolis force and emerge radially and to retain enough of the Coriolis force effect in order to obey Joy's law (Figure 6(b) of Paper I). It is rather surprising that these flux tubes also rise sufficiently slowly so

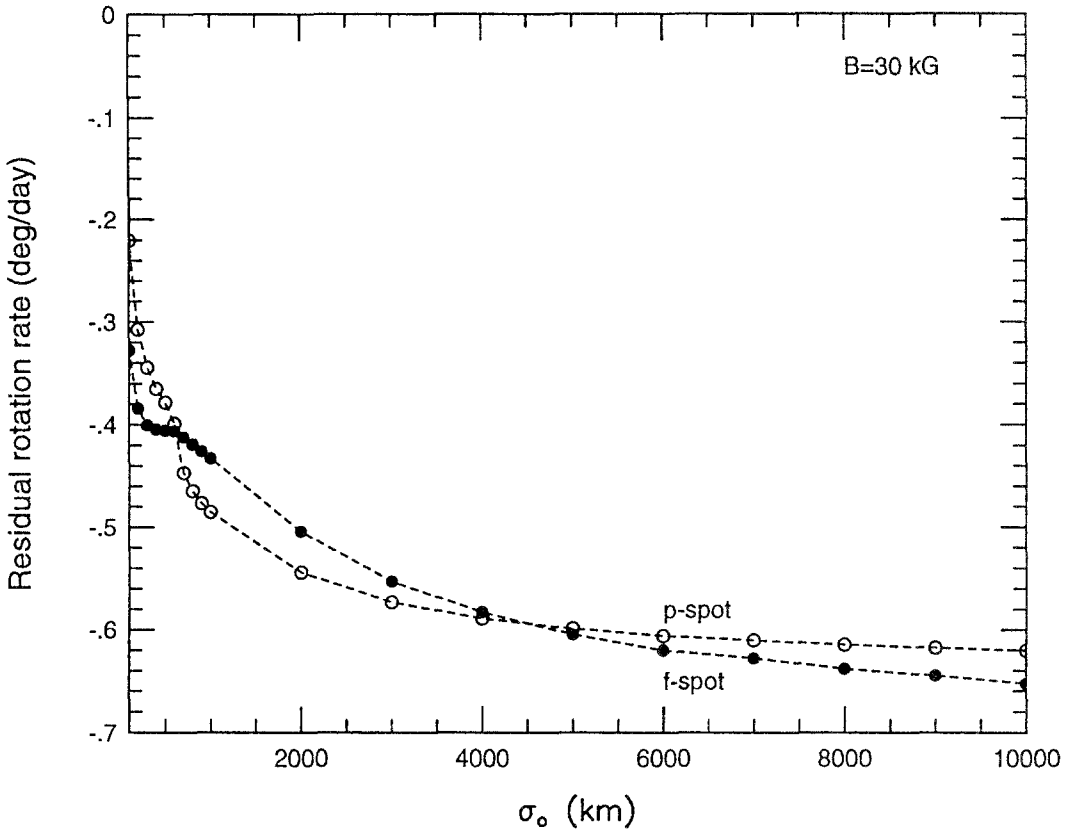

Fig. 4c. Same as Figure 4(a) for 30-kG flux tubes.

that the Coriolis force evacuates their p-legs to develop an asymmetry in the loop which makes them rotate faster than the surrounding plasma, show the right size dependences of the rotation velocity, have the p-legs rotate faster than the f-legs and also mimic the observed differential rotation profiles. This clearly strengthens the claim by Paper I and D'Silva and Howard (1993), that the fields at the bottom of the convection zone that are responsible for producing the BMRs we see, should be in the range of 60 to 160 kG. It should be noted that all the calculations are compared with sunspots in growing sunspot groups, because these calculations are for rising flux tubes. The decaying sunspot groups have an entirely different story to tell; for example, the f-spots rotate faster than the p-spots by 3%, opposite to that of the growing sunspot groups (see Paper II). We have yet to understand the dynamics of the decay of sunspots in order to understand their behavior (Howard and D'Silva, 1994).

It seems more or less clear that fields stronger than 160 kG, in particular megagauss fields are not responsible for producing the BMRs. These fields, though they

emerge radially, disobey Joy's law by having tilts much smaller than the observed values. In this paper we have shown that, in addition, they show differential velocity profiles grossly different from the observed profiles and also do not show the decrease in rotation velocity with increasing flux tube size which is observed.

Acknowledgements

The sunspot data were generated in collaboration with Dr Peter A. Gilman of the National Center for Atmospheric Research. SDS wishes to thank Arnab Rai Choudhuri for discussions and for lending his code, and is grateful to the Smithsonian Institution for travel support, which greatly facilitated this work.

References

Choudhuri, A. R.: 1989, *Solar Phys.* **123**, 217.
Choudhuri, A. R. and D'Silva, S.: 1990, *Astron. Astrophys.* **239**, 326.
Choudhuri, A. R. and Gilman, P. A.: 1987, *Astrophys. J.* **316**, 788.
Christensen-Dalsgaard, J. and Schou, J.: 1988, in V. Domingo and E. J. Rolfe (eds.), *Seismology of the Sun and Sun-like Stars*, ESA SP-286, p. 149.
D'Silva, S.: 1993, *Astrophys. J.* **407**, 385.
D'Silva, S. and Choudhuri, A. R.: 1991, *Solar Phys.* **136**, 201.
D'Silva, S. and Choudhuri, A. R.: 1993, *Astron. Astrophys.* **272**, 621 (Paper I).
D'Silva, S. and Howard, R.: 1993, *Solar Phys.* **148**, 1.
Dziembowski, W. A., Goode, P. R., and Libbrecht, K. G.: 1989, *Astrophys. J.* **337**, L53.
Fan, Y., Fisher, G. H., and DeLuca, E. E.: 1993, *Astrophys. J.* **405**, 390.
Foukal, P.: 1972, *Astrophys. J.* **173**, 439.
Gilman, P. A. and Foukal, F.: 1979, *Astrophys. J.* **229**, 1179.
Gilman, P. A. and Howard, R.: 1985, *Astrophys. J.* **295**, 233.
Hale, G. E., Ellerman, F., Nicholson, S. B., and Joy, A. H.: 1919, *Astrophys. J.* **49**, 153.
Howard, R. F.: 1990, *Solar Phys.* **126**, 299.
Howard, R. F.: 1991, *Solar Phys.* **136**, 251.
Howard, R. F.: 1992a, *Solar Phys.* **142**, 47 (Paper I).
Howard, R. F.: 1992b, *Solar Phys.* **142**, 233.
Howard, R. F. and D'Silva, S.: 1994, in preparation.
Howard, R. F., Gilman, P. A., and Gilman, P. I.: 1984, *Astrophys. J.* **283**, 385.
Moreno-Insertis, F.: 1986, *Astron. Astrophys.* **166**, 291.
Snodgrass, H. B., Howard, R., and Webster, L.: 1984, *Solar Phys.* **90**, 199.
Spruit, H. C.: 1981, *Astron. Astrophys.* **98**, 155.
Wang, Y.-M. and Sheeley, N. R.: 1989, *Solar Phys.* **124**, 81.
Wang, Y.-M. and Sheeley, N. R.: 1991, *Astrophys. J.* **375**, 761.
Yoshimura, H.: 1971, *Solar Phys.* **18**, 417.